Heliyon 9 (2023) e18063

Contents lists available at ScienceDirect

Heliyon

journal homepage: www.cell.com/heliyon

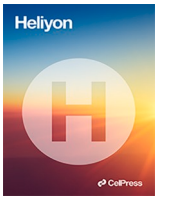

Estimation of interaction parameters in the Al-Ga-As-Sn-Bi system

Vladimir Khvostikov *, Olga Khvostikova, Nataliia Potapovich, Alexey Vlasov, Roman Salii

Ioffe Institute, Politechnicheskaya 26, St. Petersburg, 194021, Russia

ARTICLE INFO

Keywords:
Crystal growth
Thermodynamic modeling
Ga–Bi melt
Hall data

ABSTRACT

The development of GaAs based high power side-input photovoltaic converters requires thick (50–100 μm) transparent gradient refraction layers that can be grown by liquid phase epitaxy. Such thick layers can also be used in LED structures. To solve the problem of $Al_xGa_{1-x}As$ conductivity reduction at the x∼40% point a five-component, Al-Ga-As-Sn-Bi system is proposed. The interaction parameters in the liquid phase (*αij*) in the Al-Ga-As-Sn-Bi system are determined within the framework of a quasi-regular solutions model. For an $Al_xGa_{1-x}As$ solid solution growing from a Ga-melt containing 10 at.% of Bi (as a neutral solvent) and 15 at.% of Sn (as an n-type dopant), liquidus and solidus isotherms for 900 °C are modeled based on the calculated *αij*. Satisfactory agreement between calculated and experimental data has been obtained. Hall data show that AlGaAs layers grown from Bi-containing melts have n-type conductivity. Doping by tin during growth from mixed Ga–Bi melts makes it possible to increase the electron concentration in the AlGaAs layer.

1. Introduction

The traditional configuration of a photovoltaic (PV) converter implies the input of radiation through a frontal window located parallel to the p-n junction plane. This approach has fundamental limitations on the power density of the incident radiation. The input of radiation in the direction parallel to the p-n junction (side input) opens up opportunities to break through the limits, but requires a waveguide layer with a thickness of at least 50 μm (wider than a multimode fibre core diameter). Such an approach is realized in the GaInAs/InP system where the InP substrate can act as a waveguide [1]. In the GaAs-AlGaAs system discussed here a wide-gap AlGaAs layer acts as a waveguide. An efficient collection of light towards the p-n junction is provided by the composition gradient x=0.55–0.15 (and, correspondingly, the refractive index) [2–4]. This gradient bends the light beam towards the p-n junction.

Liquid-phase epitaxy (LPE) is the only cost-effective method of obtaining such relatively thick layers, which can also be used in high brightness infrared LEDs [5,6]. This method has another advantage: with a forced decrease in the temperature of the melt solution in the growing AlGaAs layer, a change in the aluminum content occurs due to the dependence of the aluminum segregation coefficient on crystallization temperature. Therefore, when growing a waveguide layer in the Al-Ga-As system by liquid-phase epitaxy, it is possible to create the required band gap gradient, and, as a result, the refractive index gradient of the layer.

To ensure the low Ohmic losses of the PV converter, all layers in the structure, including the substrate, except for the photoactive (diode base) n-type layer, must possess a carrier concentration of at least 5×10^{17} cm^{-3}. Group IV or group VI elements (e.g. Sn, Te, Se) can be used for this. $Al_xGa_{1-x}As$ layers grown from Ga-melts (the traditional approach) in the x=0.35–0.40 composition range

* Corresponding author.
E-mail address: vlkhv@scell.ioffe.ru (V. Khvostikov).

https://doi.org/10.1016/j.heliyon.2023.e18063
Received 20 March 2023; Received in revised form 5 July 2023; Accepted 5 July 2023
Available online 7 July 2023

demonstrate a sharp drop in the conductivity [7]. One way to solve this problem is to study the electrical properties of the $Al_xGa_{1-x}As$ alloys grown from Bi-containing melts. Bismuth is used as a neutral solvent, which is an isovalent impurity in AlGaAs. According to Refs. [8–10], an increase in the distribution coefficient of Sn and the electron concentration is observed in GaAs layers crystallized from a Bi melt. This effect can be explained by a change in the ratio of gallium and arsenic in the melt, which promotes the incorporation of Sn into the Ga sublattice, as well as by a change in the distribution coefficient of background impurities.

To date, the properties of the $Al_xGa_{1-x}As$ layers grown from a Bi-containing melt have not been studied. Phase diagrams of Al-Ga-As-Bi and Al-Ga-As-Sn-Bi were modeled only for the case of Bi- and Sn-enriched melts ($x_{Ga} \leq 10$ at.%) [11]. The purpose of this work is to find the binary interaction parameters αij in the Al-Ga-As-Sn-Bi system for modeling liquidus-solidus isotherms and, using these data, to study the possibility of increasing the doping level of the AlGaAs layer in device structures.

1.1. Theoretical basis

To model the theoretical isotherms, sufficiently accurate interaction parameters (αij) in the liquid phase are required. Interaction parameters in the Al-Ga-As-Sn system without bismuth are provided in Ref. [7]. Here, the calculation of interaction parameters in the liquid phase α_{AlBi}, α_{BiGa}, α_{AsBi}, α_{BiSn} was performed within the framework of the model of quasi-regular solutions, where the interaction parameter $\alpha ij(T)$=a-bT is a linear function of temperature. A similar approach to estimating αij was used in Refs. [12,13].

$$\alpha = \frac{T\Delta S_{fi} - \Delta H_{fi} - RT \cdot \ln x_i}{(1 - x_i)^2} = \frac{\Delta H_{fi}\left(T/T_{fi} - 1\right) - RT \cdot \ln x_i}{(1 - x_i)^2} \quad (1)$$

where the i symbol shows the i-side data of the binary phase diagram, ΔS_{fi}, ΔH_{fi} and T_{fi} – fusion entropy, enthalpy and melting point temperature of i-component, x_i – at. fraction of i-component in liquid phase at temperature T, R – universal gas constant.

To calculate the interaction parameter αij by Eq. (1), we used the i-side of the binary diagram of i-j pair, which is characterized by negligible solubility in the solid phase. Table 1 shows the segment of liquidus data of the binary diagram used to estimate αij. Ga–Bi and Al–Bi alloys have a binary diagram with immiscibility region, therefore the liquidus region for calculating αij is even more limited. Since the parameter αij is sensitive to the inaccuracy of the experimental values (T and x_i) near the melting point [12,13], this liquidus segment was not used. The enthalpy and melting temperature data of the elements required for the calculation were collected from independent sources [14–16]. To reduce the calculation error, the liquidus data of the binary diagram of each i-j pair from different sources were used [17,18,19–22]. The exception was the Ga–Bi pair, for which detailed liquidus data at x_{Bi}=0–8.5 at.% is available [23].

2. Experimental details

To check the accuracy of the derived interaction parameters, the Al-Ga-As-Sn-Bi (x_{Sn}=15%, x_{Bi}=10%) system was chosen. To compare the liquidus and solidus theoretical curves based on αij estimation, experimental isotherms were obtained at 900 °C. The temperature of 900 °C was chosen because of the need for thick layers. The maximum Sn concentration is limited to 15 at.% in the melt since higher values result in surface morphology degradation. Concentrations of x_{Sn} higher than 20 at.% do not lead to a significant increase in the doping level [7]. The content of bismuth in the melt was chosen to be 10 at.% because the solubility of arsenic decreases with increasing x_{Bi} in the melt [11]. Despite the fact that this system is considered to be five-component and because the solubility of tin and bismuth in the $Al_xGa_{1-x}As$ solid solution is negligible, the solid phase remains three-component. Bismuth acts as a neutral solvent (isovalent impurity), and tin as a dopant.

To determine the experimental data on the liquidus in the Al-Ga-As-Bi-Sn system, we used the method of melt saturation with arsenic from the GaAs substrate at a constant temperature. To do this, in a slide graphite boat, a melt (5 mm height) of a given composition for bismuth and tin (x_{Bi}=10 at.%, x_{Sn}=15 at.%, x_{Ga}~70 at.%) with a variable content of x_{Al} was kept at T=900 °C for 50–60 min in contact with a GaAs substrate for saturation with arsenic (Fig. 1a). The substrate and melt components were weighed on a Radwag electronic analytical balance with an accuracy of 0.01 mg. The solubility of arsenic (x_{As}) was determined from the weight loss of the GaAs (100) substrate during the saturation stage and ranged from tens to several hundreds of milligrams, depending on the aluminum content in the melt. The design of the boat ensured the complete removal of the melt from the substrate surface. The process was carried out in a quartz reactor in a flow of purified hydrogen.

The experimental values of the solidus curve (x) were determined by the crystallization of the $Al_xGa_{1-x}As$ layer (2–3 μm) from the melt saturated (Fig. 1b) according to the obtained liquidus. The composition of the layers was estimated by means of Raman spectroscopy, which is a fast and reliable method for AlGaAs alloys with an accuracy of 1–2% [24].

Table 1
Thermodynamic parameters of i-j pairs.

i-j pair	The liquidus segment of the binary diagram used to calculate αij	T_{fi}, K [14–16]	ΔH_{fi}, J/mole [14–16]
Al-Bi [17,18]; Al side liquidus	0.54 <x_{Al}< 16 at.%; 623 < T < 923 K	933.3	10,790
Bi-Ga [23]; Bi side liquidus	0.22 <x_{Bi}< 8.5 at.%; 373 < T < 493 K	544.3	11,300
As-Bi [19,20]; As side liquidus	0.5< x_{As}< 80 at.%; 600 < T < 923 K	1090	27,700
Bi-Sn [21,22]; Bi side liquidus	43 <x_{Bi}< 80 at.%; 423 < T < 498 K	544.3	11,300

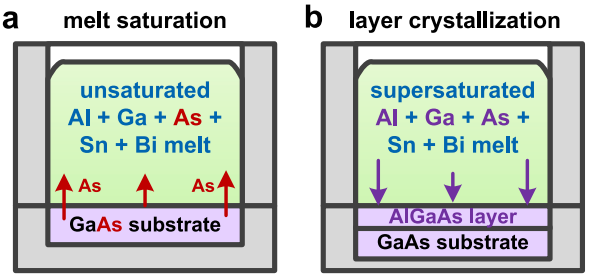

Fig. 1. Scheme of melt saturation (a) and layer growth (b) stages.

3. Results and discussion

Fig. 2 shows the calculated values of the interaction parameters α_{AlBi}, α_{BiGa}, α_{AsBi}, α_{BiSn} according to Eq. (1). Each parameter is calculated in the corresponding temperature range of the liquidus segment (Table 1). Temperature coefficients (a, b) of each interaction parameter αij can be found in Fig. 2.

The values of the interaction parameters α_{AlBi}, α_{BiGa}, α_{AsBi}, α_{BiSn} found in the literature are collected in Table 2. The discrepancy between the data may be due to the use of different calculation models of αij. In Refs. [10,25] the interaction parameters were determined within the framework of the regularly associated solution model. The interaction parameters in appendix [26] were found by fitting from data of *N*-shaped GaAs-Bi liquidus. In Ref. [11] the authors do not provide a model for estimating αij nor do they confirm the calculated parameters with experimental data in the Al-Ga-As-Bi-Sn system. The phase diagrams in Ref. [11] were modeled in the Bi-enriched corner ($x_{Ga} \leq 10$ at.%). When constructing theoretical isotherms for the Ga-enriched corner (Al-Ga-As-Sn-Bi, T=900 °C, x_{Bi}=10 at.%, x_{Sn}=15 at.%, $x_{Ga} \geq 70$ at.%) using αij from Ref. [11] a discrepancy with the experimental data of more than 30% was observed. We used binary diagrams refined most recently, which can also affect the difference between the published αij and those obtained in this work.

Based on the obtained interaction parameters (Fig. 2), liquidus and solidus curves were modeled assuming that the extrapolated αij values remain unchanged for a temperature of 900 °C. The theoretical liquidus and solidus isotherms were determined using a computer program based on the equations from appendix A (Additional information). Thermodynamic parameters for the calculation of the Al-Ga-As-Sn-Bi phase diagram are given in ibidem. Fig. 3 presents the calculated solidus (curve 1) and the experimental points (hollow dots) of $Al_xGa_{1-x}As$ alloy composition vs the aluminum content in the liquid phase. The calculated liquidus (Fig. 3, curve 2a) and the experimental arsenic solubility points (solid dots) are also marked there.

The best agreement between the experimental data (solid dots on Fig. 3) and the calculated liquidus (curve 2 b) occurs with the value of α_{AsBi}=4800-3.3T. In this case, all other calculated interaction parameters remain the same. Changing the parameter from α_{AsBi}=4800-5.3T to α_{AsBi}=4800-3.3T has practically no effect on the solidus profile. Final αij values that provide the best agreement between the calculated and the experimental data are collected in Table 2.

Table 3 presents the data for tin doping, where the results for LPE are collected [7,27]. For Hall measurements the *n*-AlGaAs layers (x=0.2–0.24) were grown by the LPE technique with saturation at 900 °C in a piston graphite boat on the semi-insulating GaAs substrate. The thickness of the grown layers was 3–6 μm, since a greater thickness x of $Al_xGa_{1-x}As$ deviates from the required composition. Hall mobility correlates with the drift mobility through the Hall factor (r) [28]. To avoid uncertainty, we chose the

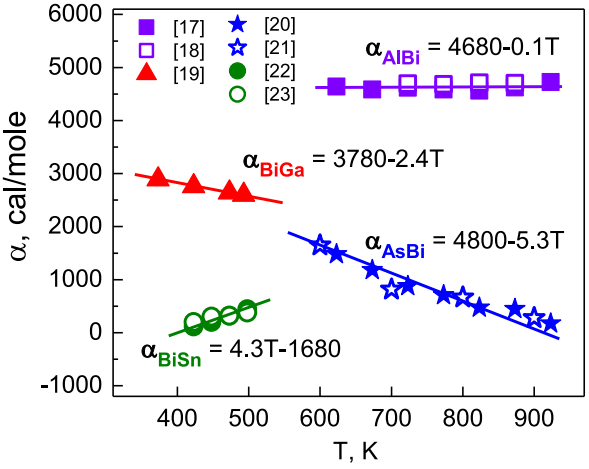

Fig. 2. Interaction parameters calculated for *i-j*-pairs.

Table 2
Interaction parameters in the Al-Ga-As-Sn-Bi system.

αij, cal/mole	α_{AlBi}	α_{BiGa}	α_{AsBi}	α_{BiSn}
Published data	2000 + T [11]	6650-6.5T [11] 3350–3.68T [25] 3420 + 0.44T [26]	6000-T [11] 10,875–8.22T [10] 3840–3.14T [26]	2000 [11]
Data of this work	4680-0.1T	3780-2.4T	4800-3.3T	4.3T-1680

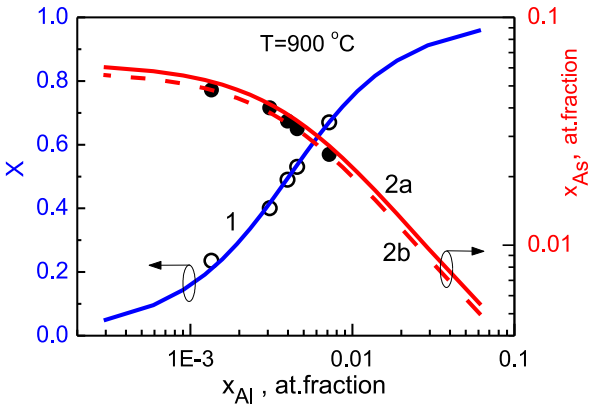

Fig. 3. Solidus (curve 1) and experimental data for Al-Ga-As-Sn-Bi system (hollow dots). Liquidus (curve 2a – calculation based on α_{AsBi}=4800-5.3T, curve 2 b – calculation based on α_{AsBi}=4800-3.3T) and experimental data (solid dots).

Table 3
Hall data of $Al_xGa_{1-x}As$ layers.

melt	x_{Bi}, %	x_{Sn}, %	n, cm^{-3}	T_{growth}, °C	Ref.
Ga	0	0	p-type	850	[27]
Ga	0	0	p-type	900	data of this work
Ga–Bi	10	0	$(2–3)\cdot10^{16}$	900	data of this work
Ga	0	15	$(5–6)\cdot10^{17}$	800	[7]
Ga	0	15	$(2–3)\cdot10^{17}$	850	[27]
Ga–Bi	10	15	$9\cdot10^{17}$	900	data of this work

x=0.2–0.24 composition range for doping comparison with r ≅ 1. The carrier concentration was obtained by the four-probe modified van der Pauw method. To do this, we used the installation Ecopia HMS-3000 for measuring the parameters of semiconductor materials on the Hall effect. It is known that the surface of a semi-insulating GaAs substrate changes its conductivity to p-type at temperatures above 900 °C [29]. To avoid additional errors in Hall measurements the semi-insulating substrate was etched (3–6 s) with an arsenic-unsaturated melt before growing the AlGaAs layer to remove the inverse surface layer.

As can be seen from Table 3, undoped AlGaAs layer, grown from the Ga–Bi melt (without Sn) possesses n-type conductivity, while the use of pure Ga melt reveals the p-type. Thus, adding bismuth to the melt makes it possible to avoid the inversion of the conduction type of AlGaAs layer. The growth from the mixed Ga–Bi melt with added Sn leads to a corresponding increase in the doping level. A similar effect was observed for GaAs layers grown from bismuth melt [8,9]. Bismuth increases arsenic activity (effective concentration). Changing the ratio in the liquid phase of III/V groups contributes to the reduction of acceptor native defects (V_{As}, Ga_{As}, C_{As}) [10]. Replacing the solvent (Ga by Bi) during the crystallization of undoped GaAs makes it possible to obtain low-compensated layers even at a high growth temperature T ~ 900 °C [10], where the level of doping with background impurities of the growing layer increases. Since carbon (p-type dopant) is the main background impurity in liquid phase epitaxy with the use of a graphite boat, the task of reducing the doping level of this impurity becomes especially important when growing relatively thick AlGaAs structures, because melt homogenization and layer crystallization occur at sufficiently high temperatures T > 900 °C. Thus, the use of mixed Ga–Bi melts provides an opportunity to reduce background doping and ohmic losses (Table 3).

4. Conclusion

Based on the *αij* values obtained, theoretical isotherms of the five-component system (Al-Ga-As-Sn-Bi, T=900 °C, x_{Sn}=15 at.%, x_{Bi}=10 at.%) were modeled and confirmed by experimental data. AlGaAs layers grown from Ga–Bi melts did not change the type of conductivity even without Sn. Doping by tin of $Al_xGa_{1-x}As$ solid solutions from mixed melts leads to increase n-type conductivity in grown layer. This study is of high practical importance for the growth of highly efficient side-input photovoltaic converters of laser

radiation [2–4,30] and high brightness infrared LEDs [5,6]. The use of Bi-containing melts reduces background doping, which makes it possible, by using Sn, to keep the doping level constant in a thick (more than 50 μm) gradient composition AlGaAs layers to ensure low Ohmic losses of some optoelectronic devices.

Author contribution statement

Vladimir Khvostikov, Olga Khvostikova: Conceived and designed the experiments; Performed the experiments; Analyzed and interpreted the data; Wrote the paper.

Nataliia Potapovich, Alexey Vlasov, Roman Salii: Performed the experiments; Analyzed and interpreted the data; Contributed reagents, materials, analysis tools or data.

Data availability statement

No data was used for the research described in the article.

Additional information

Supplementary content related to this article has been published online at.

Declaration of competing interest

The authors declare that they have no known competing financial interests or personal relationships that could have appeared to influence the work reported in this paper.

Acknowledgments

This work was supported by the Russian Science Foundation (https://rscf.ru/en/project/22-19-00057/) under Grant 22-19-00057.

Appendix A. Supplementary data

Supplementary data to this article can be found online at https://doi.org/10.1016/j.heliyon.2023.e18063.

References

[1] T. Nagatsuma, H. Ito, T. Ishibashi, High-power RF photodiodes and their applications, Laser Photon. Rev. 3 (1–2) (2009) 123–137, https://doi.org/10.1002/lpor.200810024.
[2] V. P Khvostikov, P.V. Pokrovskiy, O.A. Khvostikova, A.N. Panchak, V.M. Andreev, High-efficiency AlGaAs/GaAs photovoltaic converters with edge input of laser light, Tech. Phys. Lett. 44 (2018) 776–778, https://doi.org/10.1134/S1063785018090079.
[3] A. Panchak, V. Khvostikov, P. Pokrovskiy, AlGaAs gradient waveguides for vertical p/n junction GaAs laser power converters, Opt Laser. Technol. 136 (2021), 106735, https://doi.org/10.1016/j.optlastec.2020.106735.
[4] V.P. Khvostikov, A.S. Vlasov, P.V. Pokrovskiy, O.A. Khvostikova, A.N. Panchak, E.P. Marukhina, N.A. Kalyuzhnyy, V.M. Andreev, Characterization of ultra high power laser beam PV converters, AIP Conf. Proc., Fes, Morocco 2149 (2019), 080003, https://doi.org/10.1063/1.5124213.
[5] V. Zinovchuk, O. Malyutenko, V. Malyutenko, A. Podoltsev, A. Vilisov, The effect of current crowding on the heat and light pattern in high-power AlGaAs light emitting diodes, J. Appl. Phys. 104 (2008), 033115, https://doi.org/10.1063/1.2968220.
[6] H. Kitabayashi, K. Ishihara, Y. Kawabata, H. Matsubara, K. Miyahara, T. Morishita, S. Tanaka, Development of super high brightness infrared LEDs, SEI Tech. Rev. 72 (2011) 86–89. https://sumitomoelectric.com/sites/default/files/2020-12/download_documents/72-12.pdf.
[7] M.B. Panish, Phase equilibria in the system Al–Ga–As–Sn and electrical properties of Sn-doped liquid phase epitaxial AlxGa1−xAs, J. Appl. Phys. 44 (1973) 2667–2675, https://doi.org/10.1063/1.1662631.
[8] N.A. Yakusheva, G.M. Beloborodov, Doping of GaAs with tin in the process of liquid-phase epitaxy from bismuth melt, Izv. Acad. Nauk SSSR Inorg. Mater. 26 (1990) 9–13 (in Russian).
[9] N.A. Yakusheva, V.G. Pogadaev, Doping of GaAs with donor impurities Te and Sn during liquid phase epitaxy from mixed gallium bismuth melts, Cryst. Res. Technol. 27 (1992) 21–30, https://doi.org/10.1002/crat.2170270104.
[10] N.A. Yakusheva, K.S. Zhuravlev, S.I. Chikichev, O.A. Shegay, Liquid phase epitaxial growth of undoped gallium arsenide from bismuth and gallium melts, Cryst. Res. Technol. 24 (1989) 235–246, https://doi.org/10.1002/crat.2170240221.
[11] V.S. Antoschenko, Yu V. Francev, O.A. Lavrischev, E.V. Antoschenko, Investigation of phase equilibriain the quinary system Sn-Bi-Ga-Al-As, KazNU Bull. Phys. series 44 (2013) 11–17 (in Russian), https://bph.kaznu.kz/index.php/zhuzhu/article/view/65.
[12] C.D. Thurmond, M. Kowalchik, Germanium and silicon liquidus curves, Bell Syst. Tech. J. 39 (1960) 169–204, https://doi.org/10.1002/j.1538-7305.1960.tb03927.x.
[13] J. Safarian, L. Kolbeinsen, M. Tangstad, Liquidus of silicon binary systems, Metall. Mater. Trans. B 42 (2011) 852–874, https://doi.org/10.1007/s11663-011-9507-4.
[14] ([online available] Material Properties), https://material-properties.org, 2023.
[15] ([online available] Material Properties), https://periodictable.com, 2023.
[16] A.T. Dinsdale, SGTE data for pure elements, Calphad 15 (1991) 317–425, https://doi.org/10.1016/0364-5916(91)90030-N.
[17] H. Okamoto, Supplemental literature review of binary phase diagrams: Al-Bi, Al-Dy, Al-Gd, Al-Tb, C-Mn, Co-Ga, Cr-Hf, Cr-Na, Er-H, Er-Zr, H-Zr, and Ni-Pb, J. Phase Equilibria Diffus. 35 (2014) 343–354, https://doi.org/10.1007/s11669-014-0300-3.

[18] M. Paliwal, I.H. Jung, Thermodynamic modeling of the Al–Bi, Al–Sb, Mg–Al–Bi and Mg–Al–Sb systems, Calphad 34 (2010) 51–63, https://doi.org/10.1016/j.calphad.2009.11.004.
[19] H. Okamoto, M.E. Schlesinger, E.M. Mueller, in: Rev (Ed.), Alloy Phase Diagram Committee, ASM Metals, Park, OH, 2016, pp. 337–338, https://doi.org/10.31399/asm.hb.v03.9781627081634.
[20] B. Predel, Phase Equilibria. Crystallographic and Thermodynamic Data of Binary Alloys Ac-Au – Au-Zr, IV-5A, Landolt-Börnstein, 1991, https://doi.org/10.1007/10000866_190.
[21] P.T. Vianco, J.A. Rejent, Mater. Properties of ternary Sn-Ag-Bi solder alloys: Part I - thermal properties and microstructural analysis, J. Electron. 28 (1999) 1127–1137, https://doi.org/10.1007/s11664-999-0250-4.
[22] M.H. Braga, J. Vizdal, A. Kroupa, J. Ferreira, D. Soares, L.F. Malheiro, The experimental study of the Bi–Sn, Bi–Zn and Bi–Sn–Zn systems, Calphad 31 (2007) 468–478, https://doi.org/10.1016/j.calphad.2007.04.004.
[23] A. Turchanin, W. Freyland, D. Nattland, Surface freezing in a liquid eutectic Ga–Bi alloy, Phys. Chem. Chem. Phys. 4 (2002) 647–654, https://doi.org/10.1016/S0009-2614(01)00185-3.
[24] D.J. Lockwood, Z.R. Wasilewski, Optical phonons in AlxGa1−xAs: Raman spectroscopy, Phys. Rev. B 70 (2004), 155202, https://doi.org/10.1103/PhysRevB.70.155202.
[25] A.S. Jourdan, Calculation of phase equilibria in the Ga-Bi and Ga-P-Bi systems based on a theory of regular associated solutions, Metall. Trans. B 7 (1976) 191–201, https://doi.org/10.1007/BF02654917.
[26] D.T.J. Hurle, A thermodynamic analysis of native point defect and dopant solubilities in zinc-blende III–V semiconductors, J. Appl. Phys. 107 (2010), 121301, https://doi.org/10.1063/1.3386412.
[27] X. Zhao, K.H. Montgomery, J.M. Woodall, Hall effect studies of AlGaAs grown by liquid phase epitaxy for tandem solar cell applications, J. Electron. Mater. 43 (11) (2014) 3999–4002, https://doi.org/10.1007/s11664-014-3340-x.
[28] A.K. Saxena, Hall to drift mobility ratio in Ga1−xAlxAs alloys, Solid State Commun. 39 (1981) 839–842, https://doi.org/10.1016/0038-1098(81)90526-3.
[29] A. Nouiri, Y. Sayad, A. Djemel, Study of acceptor centers in GaAs after high temperature annealing, Exp. Calculation, Phys. Stat. Sol. 0 (2) (2003) 665–668, https://doi.org/10.1002/pssc.200306208.
[30] V.P. Khvostikov, A.N. Panchak, O.A. Khvostikova, P.V. Pokrovskiy, Side-input GaAs laser power converters with gradient AlGaAs waveguide, IEEE Electron. Device Lett. 43 (2022) 1717–1719, https://doi.org/10.1109/LED.2022.3202987.